ARTICLE

Low-Temperature Exfoliated Graphenes: Vacuum-Promoted Exfoliation and Electrochemical Energy Storage

Wei Lv,[†] Dai-Ming Tang,[‡] Yan-Bing He,[†] Cong-Hui You,[†] Zhi-Qiang Shi,[†] Xue-Cheng Chen,[†] Cheng-Meng Chen,[†] Peng-Xiang Hou,[‡] Chang Liu,[‡] and Quan-Hong Yang[†,*]

[†]Key Laboratory for Green Chemical Technology of Ministry of Education, School of Chemical Engineering and Technology, Tianjin University, Tianjin 300072, China, and [‡]Shenyang National Laboratory for Materials Science, Institute of Metal Research, Chinese Academy of Sciences, Shenyang 100016, China

ABSTRACT A preheated high-temperature environment is believed to be critical for a chemical-exfoliation-based production of graphenes starting from graphite oxide, a belief that is based on not only experimental but also theoretical viewpoints. A novel exfoliation approach is reported in this study, and the exfoliation process is realized at a very low temperature, which is far below the proposed critical exfoliation temperature, by introducing a high vacuum to the exfoliation process. Owing to unique surface chemistry, low-temperature exfoliated graphenes demonstrate an excellent energy storage performance, and the electrochemical capacitance is much higher than that of the high-temperature exfoliated ones. The low-temperature exfoliation approach presents us with a possibility for a mass production of graphenes at low cost and great potentials in energy storage applications of graphene-based materials.

KEYWORDS: graphene · low temperature · high vacuum · surface chemistry · electrochemical energy storage

As a one-atom-thick two-dimensional material, graphene shows high thermal conductivity and superior mechanical and excellent electronic transportation properties.[1] Graphene-based electronic devices,[2] liquid crystal devices,[3] transparent conductive membrane,[4] and composite materials[5] have been developed and investigated. Graphene is usually prepared by mechanical exfoliation of graphite,[6] heat-treatment of SiC[7] or metal-containing carbon,[8] chemical vapor deposition (CVD) of carbon-containing gas,[9] and the reduction of graphene oxide.[10] Some other methods for producing graphenes also appear more recently, for example, electrostatic deposition[11] and chemical mechanical polishing on solid and perforated substrates,[12] microwave plasma induced gas-phase synthesis,[13] and unzipping of carbon nanotubes.[14] Membrane-shaped graphene-based macrostructures have also been extensively investigated, and many assembly methods have been reported recently.[15−20]

The exfoliation of graphene sheets from bulk graphite, through oxidation-derived intercalation−expansion and then quick removal of these oxygen groups, represents a very efficient approach for graphene materials. It is believed that a heat-treatment with a very rapid heating rate (*e.g.*, directly putting samples into a preheated furnace) is a key component for full exfoliation of graphene layers. McAllister *et al.* suggests a critical temperature of 550 °C for exfoliation of graphite oxide to occur;[21] however, experimentally, the employed treatment temperature for full exfoliation to single- or few-layered graphenes is normally above 1000 °C.[22,23] This process is energy-consuming and hard to be well controlled, and therefore the needed high temperature environment is one of big obstacles for mass production of graphene materials by the chemical approach.

It is noted that before the appearance of graphenes, by using the similar heat-promoted exfoliation technique, many attempts have been made to prepare exfoliated graphites and thermally expanded graphite oxide (TEGO) with graphite oxide and graphite intercalation compounds as starting materials.[24−29] Boehm *et al.* found that TEGO can be produced at a temperature (~400 °C) lower than the proposed critical graphene production temperature, while other researchers reported that starting from other types of intercalated graphite materials (*e.g.*, bromide-intercalated graphite), exfoliated graphite can also be produced at a temperature apparently lower than the proposed critical temperature for graphenes.[24−29] However, in these cases, the obtained samples are only partially exfoliated and still contain extensive domains of

*Address correspondence to qhyangcn@tju.edu.cn.

Received for review August 4, 2009 and accepted October 5, 2009.

Published online October 13, 2009. 10.1021/nn900933u CCC: $40.75

staked graphitic layers. The obtained samples are worm-like or accordion-like and therefore characterized by an apparently lower specific surface area (typically lower than 100 m^2/g) compared to the few-layered graphenes reported recently. In short, the expansion and exfoliation of graphite oxide and other graphite intercalation compounds may occur below the critical temperature (550 °C) proposed by McAllister *et al.*, but the graphitic layers are not completely exfoliated as occurs to the cases of recently reported graphenes which contain fully exfoliated sheets.

In this study, we report a low-temperature exfoliation approach (far lower than the normally employed and even lower than the predicted critical exfoliation temperatures) to produce graphenes. The exfoliation temperature of graphite oxide is as low as 200 °C and the exfoliation process must be accompanied with a high vacuum environment, which has never been reported before for both graphenes and TEGO. The graphene materials obtained are of high specific surface area (~1000 m^2/g based on methylene blue (MB) dye adsorption and ~400 m^2/g (S_{BET}) based on BET analyses of nitrogen cryo-adsorption method, respectively) and electrochemical capacitance up to 264 F/g (for the tenth cycle) without any post-treatments.

RESULTS AND DISCUSSION

A chemical exfoliation of graphenes involves two steps, the first resulting in fully oxidized graphite by using a modified Hummers method[30] and the second being responsible for the liberation and stabilization of individual layers. We conducted thermal analyses to examine the heating-driven structural changes of graphite oxides, and very simple thermogravimetric differential scanning calorimetry (TG−DSC) profiles are demonstrated in Figure 2a. These profiles are characterized by a marked exothermic DSC signal and correspondingly an abrupt mass-loss peak in the TG branch within a very narrow temperature range (150−250 °C). These results indicate that most of oxygen-containing functional groups bonded to graphene planes are removed in this narrow temperature range. Such a low temperature may drive oxygen to flee from the planar graphene sheets but is not enough to fully expand the graphene layers under an atmospheric pressure, and therefore, as discussed above, a preheated high-temperature environment is needed for fast expansion of graphene sheets in most cases.

The above discussion hints us that if an inner stress generated from the removal of oxygen can be reinforced at the decomposition temperature (150−250 °C) of oxygen-containing groups, a fast expansion−exfoliation of graphene layers may be achieved and few-layered graphenes can be produced at such a low temperature. We realized this process by providing a vacuum environment (<1 Pa) to achieve a fast exfoliation of graphene layers and to stabilize the individual

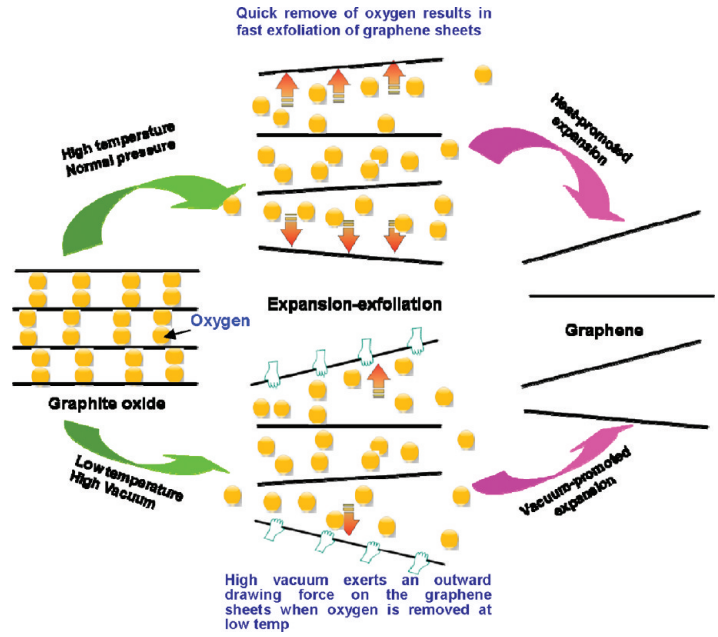

Figure 1. Schematic representation of chemical exfoliation of graphenes. (Top) High-temperature (above 1000 °C) exfoliation under an atmospheric pressure; (bottom) low-temperature (as low as 200 °C) exfoliation under high vacuum, where high vacuum introduces a negative pressure surrounding the graphene layers.

sheets. The high vacuum, accompanying the fleeing out of oxygen at a low temperature such as 200 °C, exerts an outward drawing force on the expanding graphene layers, which helps accelerate the expansion of graphene layers and results in an effective exfoliation of graphene layers (as schematically represented in Figure 1). By using this approach, few-layered graphenes have been obtained in gram scale, and the obtained sample is denoted as G-200 corresponding to the thermal treatment temperature. G-300 and G-400, thermally treated at 300 and 400 °C under high vacuum, respectively, are prepared for references.

The exfoliation degree of graphene oxide and the morphologies of these obtained graphene samples were characterized by X-ray diffraction (XRD) and microscopic observations. Figure 2b shows XRD patterns of the parent graphite, graphite oxide, and resulting graphenes. The parent graphite is characterized by a sharp (002) peak at 31.1° (Co target employed, the peak is upshifted compared to the normal cases with Cu target) with a typical interlayer spacing of 0.335 nm. The XRD pattern of graphite oxide shows a typical (002) peak located at 12.3°, corresponding to an interlayer spacing of 0.776 nm. This indicates that graphite is totally transformed into graphite oxide and most oxygen is bonded to the planar surface of graphite after the oxidization. After the low-temperature heat-treatment, the sharp peak around 12° at the XRD patterns disappears, indicating that oxygen intercalated into the interlayer spacings of graphite is largely removed during the vacuum-promoted low-temperature expansion.

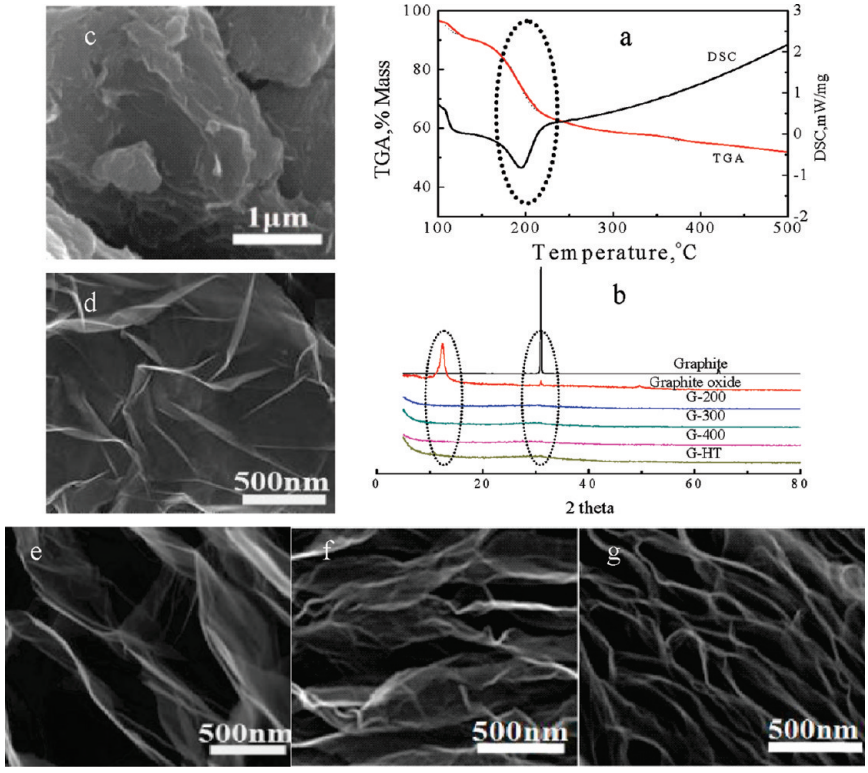

Figure 2. Characterization of a graphite oxide and the obtained graphenes: (a) TG−DSC curves of a graphite oxide; (b) XRD patterns of graphite, graphite oxide, and exfoliation-resulting graphenes; (c−g), SEM images of G-200, G-400, G-200-HT, and G-HT.

Some representative scanning electron microscopy (SEM) images of low-temperature exfoliated samples (Figure 2d,e), compared to that of parent graphite oxide (Figure 2 c), show that these layers are exfoliated to a very large extent. Note that for graphene oxide, only when a thin gold layer is sputtered onto the surface of the sample can we get a clear SEM image owing to its low electric conductivity. For the low-temperature exfoliated samples, high-resolution imaging can be easily achieved without any pretreatments, suggesting that the samples have an enhanced conductivity (In Supporting Information, a square resistance for a graphene paste electrode is presented and detailed investigations for the electrical properties are ongoing). Figure 2 panels f and g present G-200-HT (heat treating G-200 in a preheated furnace at 1000 °C) and G-HT (prepared by a normally employed high-temperature exfoliation method at 1000 °C[21]). Compared with G-200, G-200-HT and G-HT show no apparent difference from the morphological observations and adsorption measurements.

Figure 3 presents transmission electron microscopy (TEM) characterization results of G-200. Low-magnification TEM observation indicates that the samples are homogeneous micrometer-sized flakes, with low contrast, indicating the small thickness (Figure 3a,b). From the folded regions, the number of layers could be identified.[31] Figure 3 panels c, d, and e show typical high-magnification TEM images of single-, double-, and

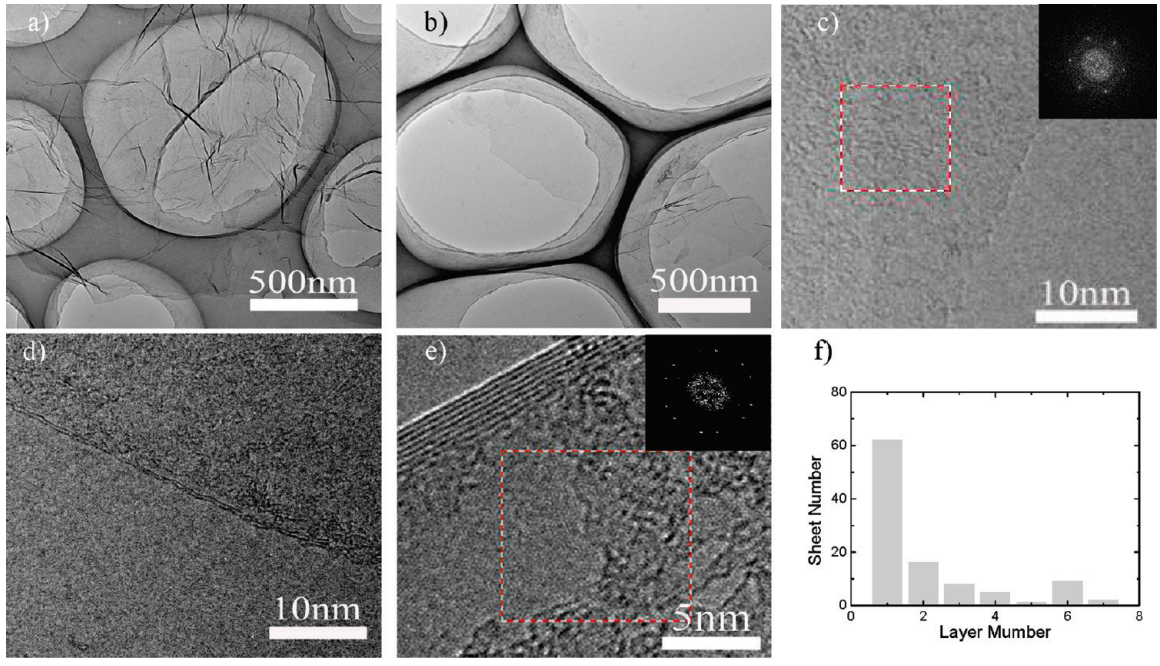

Figure 3. TEM observations of a typical low-temperature exfoliated sample, G-200: (a, b) low-magnification TEM image of G-200; (c−e) high-magnification TEM images of single-, double-, and seven-layered graphenes. Inset of panel b: FFT pattern of a single-layered graphene. Inset of panel e: FFT pattern of a seven-layered graphene. (f) Histogram of distribution of the number of graphene layers of G-200.

seven-layered graphenes, respectively. Statistics about the distribution of the number of layers reveal that the graphene sheets are few-layered (no more than seven layers) and over 60% are single-layered (Figure 3f). A fast Fourier transform (FFT) pattern of the single-layered graphene is shown as the inset in Figure 2b. Sharp diffraction spots can be seen in a hexagonal pattern, which can be indexed as a (1−110) diffraction peak, indicating the high crystallinity. Two sets of diffraction patterns can sometimes be identified in the FFT pattern of multilayered graphene (inset of Figure 3d), owing to the folded layers with different crystalline orientations. These results indicate that the obtained material is a mixture of single-layered graphene (SLG) and few-layered graphene (FLG), with SLG dominating. We further characterized the thin-layered graphene by using AFM after fully sonicating these sheets with the aid of surfactant (sodium dodecyl sulfate, $NaC1_2H_{25}SO_4$, abbreviated as SDS), and it is indicated that over 60% of observed individual sheets are of the thickness below 1.2 nm. Considering the presence of SDS surrounding the graphene sheets,[32] most of these sheets are believed to be single-layered. Figure 4a presents a typical AFM image, where three graphene sheets (circled part) are identified to be roughly overlayered with each other, and it is clearly seen from the corresponding contour profile (Figure 4b) that the one-layer part has a depth of 0.78 nm, the two-layers part has a depth of 1.55 nm, and the three-layers part depth is 2.36 nm.

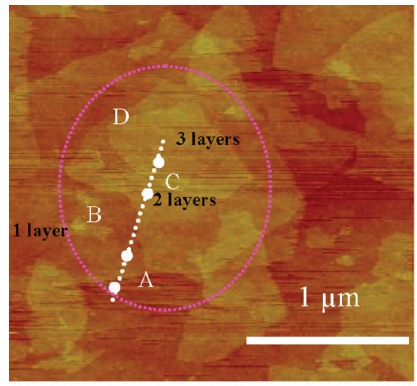

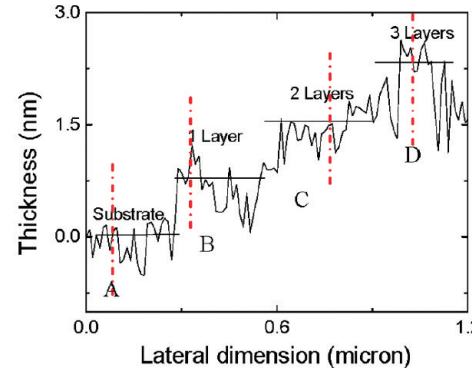

Figure 4. (Left) AFM ichnography and (right) cross-section contour of G-200 dispersed with the aid of a surfactant (SDS).

Graphene layers tend to interact with each other to form aggregated structures (as can be seen in SEM images shown in Figure 2), which cannot be ignored when considering some potential applications of graphene-based macroscopic materials (like energy storage applications). We conducted nitrogen adsorption and atomic force microscopy (AFM) measurements to probe the aggregated texture in details. Figure 5a shows N_2 cryo-adsorption isotherms of G-200, G-300, and G-400, and obviously all three samples are characterized by type II isotherms and possess hysteresis loops of type H3. The S_{BET} values of G-200, G-300, and G-400 are 368, 370, and 382 m^2/g, respectively. For different expansion temperatures, the morphologies and surface area of graphene do not show apparent differences, indicating that the temperature as low as 200 °C is enough for the expansion−exfoliation process under a high vacuum environment. The type II isotherm indicates that no micropores or small mesopores exist in the samples, whereas the type H3 hysteresis loop at relatively high pressure suggests that there exist asymmetrically slit-shaped pores of a large pore size. Considering the characteristics of the graphene materials, it is proposed that the adsorption occurs on the surface of graphene sheets, which are overlayered with each other and constitute large pores contributing to the hysteresis loops. Figure 5b schematically represents a proposed model for the aggregated structure of

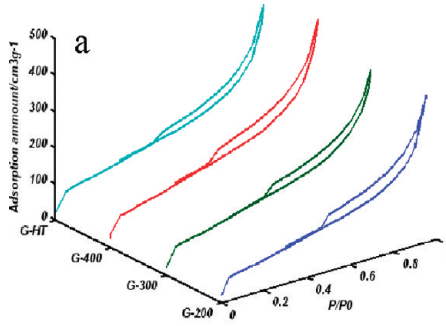

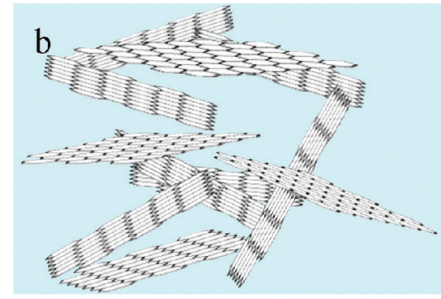

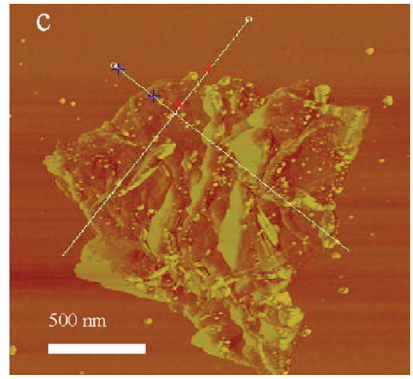

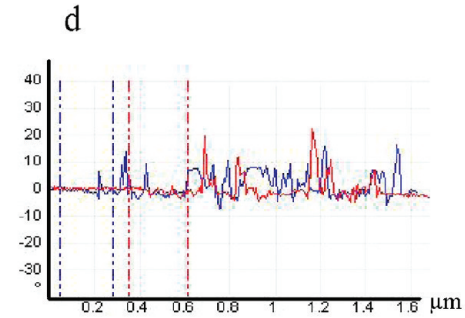

Figure 5. Characterization of aggregation state of graphenes: (a) N_2 adsorption isotherms of G-200, G-300, G-400, and G-HT at 77 K; (b) schematic representation of a graphene aggregate; (c) AFM phase image and phase-angle profile of a slightly sonicated G-200 aggregate.

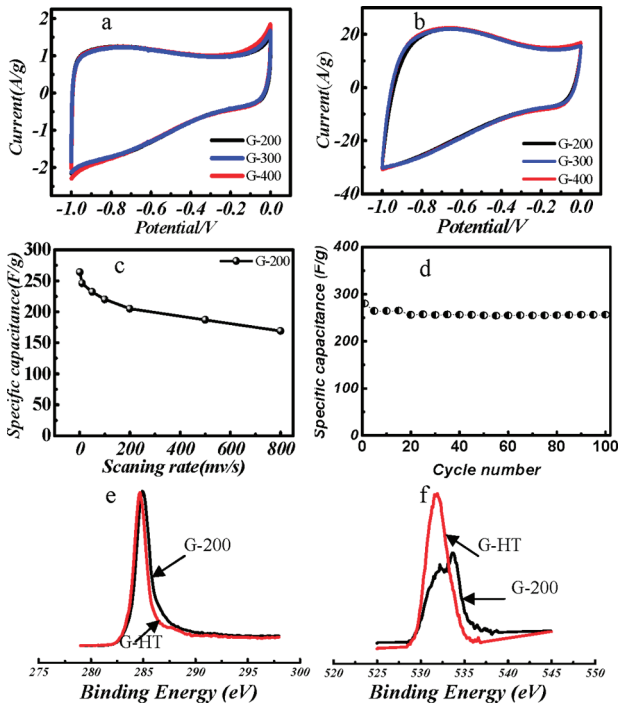

Figure 6. Electrochemical performance (a−d) and surface chemistry (e, f) of low-temperature exfoliated graphenes. Cyclic voltammetry curves of G-200, G-300, and G-400 with the scanning rates of 10 mV/s (a) and 200 mV/s (b); (c) specific capacitance of G-200 against scanning rate with 30% KOH solution as an electrolyte; (d) cycling performance of G-200 (current density: 100 mA/g); (e) C_{1s} and (f) O_{1s} XPS profiles of G-200 and G-HT.

graphenes, where graphene layers interact with each other to form an open pore system, through which electrolyte ions easily access the surface of graphene to form electric double layers. The unique open-pore system avoids the dynamic resistance of electrolyte ions within smaller pores, suggesting that graphene-based electrode materials will possibly show good power capability. To further probe the aggregate structure, we conducted atomic force microscopy (AFM) observation on the slightly sonicated sample (not changing the aggregate state substantially) on a freshly cleaved mica surface. Figure 5c) presents a typical AFM phase image of a G-200 aggregate, where quite a lot of graphene sheets are observed to be roughly overlayered with each other. It can be clearly seen from Figure 5d that isolated graphene sheets are in different phase angles (0−30°) against the mica substrate surface, providing a direct evidence for the random overlayering of graphene sheets. The random overlayering of graphene sheets does not lay great hurdles for liquid adsorbates like MB at room temperature but hinder the nitrogen diffusion onto part of the graphene surface at the cryo-temperature (77 K), which is a possible reason for the difference in specific surface area value obtained by gas and liquid adsorption.

Electrochemical properties of the low-temperature exfoliate samples were measured both with an aqueous system (the results presented in Figure 6) and an organic system (the results presented in Supporting Information). On the basis of the charge−discharge measurements, both with the current density of 100 mA/g, the capacitances for aqueous system and organic system (both for tenth cycle) are, respectively, 264 and 122 F/g and much higher than those of steam-activated phenolic-based porous carbons as a standard carbon sample (activation temperature: 850 °C) with specific surface area of 1200 m^2/g (capacitances for aqueous and organic system are 119 and 55 F/g, respectively). Figure 6 panels a and b show cyclic voltammetry (CV) measurement results (aqueous system) of G-200 at the scanning rates of 10 and 200 mV/s, respectively. At a relatively low scanning rate, the CV curves exhibit typical rectangular shape, indicative of good charge propagation at the electrode surface following the electric double layer charging mechanism. The open porous texture of the present materials is characterized by a very low internal resistance, which is as low as 0.15 Ω (aqueous system) from the electrical impedance spectroscopy (EIS). The low internal resistance is consistent with the fact that at a scanning rate as high as 200 mV/s, the CV curve still shows a rectangular shape with small distortion, indicating that the graphene samples show a good power capability. The specific capacitance of G-200 against the scanning rate is shown in Figure 6c and decreases with the increase of the scanning rate. When the scanning rate increases to 800 mV/s, the capacitance still keeps a relatively high value of 169 F/g, 65% of the highest capacitance (262 F/g at the scanning rate of 1 mV/s), further indicating good power capability. The electrochemical behaviors of G-200, G-300, and G-400 are quite similar at different scanning rates, and the capacitances at the scanning rate of 10 mV/s are 260, 269, and 279 F/g, respectively. The low-temperature exfoliated samples apparently have higher capacitance than high-temperature exfoliated samples[33] and reduced graphene oxide.[34] The capacitances of G-200-HT (~350 m^2/g, based on gas adsorption measurement) and G-HT (360 m^2/g, based on gas adsorption measurement) are 80 and 120 F/g, respectively. With the specific surface area and oxygen fraction similar to low-temperature samples (G-200), the two high-temperature samples show apparently lower electrochemical capacitance than the low-temperature ones, which suggests that different surface chemistry leads to entirely different electrochemical behaviors. The low-temperature samples are also characterized by good cycling performance as shown in Figure 6d and until the hundredth cycle, the capacitance is still up to 256 F/g. The continued cycling measurement is ongoing to measure the cycling performance with prolonged period and real application environment.

The X-ray photoelectron spectroscopy (XPS) measurements show that the low-temperature exfoliated samples (C/O ratio of G-200, 10:1) have a slightly larger fraction of oxygen compared to the samples obtained

by high-temperature approach (C/O ratio of G-HT, 11:1). Interestingly, the XPS results (Figure 6e,f) indicate an apparent difference between the low- and high-temperature samples in surface chemistry. In the O_{1s} spectrum, only one peak (531.8 eV) appears for G-HT while two peaks (531.8 and 533.6 eV) appear for G-200, which indicates that low-temperature samples are characterized by more types of oxygen-containing groups than high-temperature samples. The first peak (531.8 eV) is related to C═O-type oxygen (carbonyl, −COOR in ester) while the second peak (533.6 eV) is due to the presence of C−OH (in carboxyl or hydroxyl group) or C−O−C-type oxygen (in ether).[35,36] The apparent differences in surface chemistry of two types of graphene samples results in a big contrast in the electrochemical performance. Research is now ongoing to further identify the impact of different surface chemistries on electrochemical behaviors.

CONCLUSIONS

In summary, few-layered graphenes have been produced in gram scale by a low-temperature (exfoliation temperature as low as 200 °C) chemical exfoliation approach under a negative pressure environment (high vacuum). This approach is facile, low cost (low energy consumption), and easy to be scaled up for mass production of graphenes. The produced graphenes show great potential in electrochemical energy storage with the advantages of both high capacitance and excellent power capability due to their fully accessible surface and unique surface chemistry.

EXPERIMENTAL SECTION

Preparation of Graphite Oxide. Graphite oxide was prepared by a modified Hummers method.[30] While agitation was maintained, 10 g of graphite powder (carbon content >98 wt %) and 5 g of sodium nitrate were mixed with 230 mL of 98 wt % sulfuric acid in an ice-bath. A 30 g portion of potassium permanganate was slowly added, and the mixture was kept at 274 K for 2 h with continuous agitation. Then the mixture was transferred into the water bath and kept at 308 ± 2 K for 30 min, producing an odorous gas emission. A 460 mL portion of deionized water was gradually added into the mixture, and during this process the temperature was kept lower than 373 K by controlling the rate of water addition. The temperature of the water bath was raised up to 371 K, and the reaction was kept for 3 h in order to increase the oxidation degree of graphite−oxide product. The resulting bright yellow suspension was diluted and further treated by 30 mL of 30% H_2O_2 solution, followed by centrifugation and washing to clean out remnant salt. The wet graphite−oxide was dewatered by vacuum drying (323 K, −0.08 MPa) for 48 h.

Exfoliation of Graphite Oxide. Exfoliation of graphite oxide was achieved by a low-temperature expansion under high vacuum. The as-prepared graphite oxide was put into a quartz tube that was sealed at one end and was stoppered at the other end, through which the reaction tube was connected to the high vacuum pump. The tube was heated at the rate of 50 °C/min under a high vacuum (<1 Pa). At about 195 °C, an abrupt volume change was observed. To remove the superabundant functional groups, the graphite oxide was kept at 200 °C for 5 h and a high vacuum was maintained (below 1 Pa) during the heat treatment. The produced graphene sample was denoted as G-200. G-300 and G-400 were also obtained using a similar method, and the only differences were heating temperature, respectively, with 300 and 400 °C.

Sample Chacterization. XRD measurements were conducted at room temperature using specular reflection mode (Co Kα radiation, λ=0.77889 nm, D8 Advance, PANAlytical, Holland). AFM observation was conducted for the slightly sonicated samples on freshly cleaved mica surfaces (tip mode, frequency = 0.803 Hz, Veeco NanoScope IIIa Multimode, DI, USA). SEM and TEM observations are conducted uisng Nova NanoSEM 430, FEI and JEOL 2010F, respectively. Nitrogen adsorption was measured by using BEL mini-instrument, and the specific surface area was obtained by Brunauer−Emmett−Teller (BET) analyses of the adsorption isotherm. The surface area of graphene was also measured by a methylene blue (MB) adsorption method, where MB dye was employed as a molecular probe for the measurement of the adsorption amount and a UV−vis spectroscopy is used to measure the concentration change of MB before and after the adsorption by graphene.[21]

Electrochemical Measurements. Electrochemical properties of graphenes were measured with an aqueous system (electrolyte: 5.5 M KOH) and an organic system (electrolyte: $MeEt_3NBF_4$(AN)), respectively, and two-electrode systems were employed for the measurements (the cell configuration and a photography for a coin-type test cell are presented in the Supporting Information). CV curves (scanning rates varying from 1 to 800 mV/s) and EIS profiles were measured with an electrochemistry workstation (Princeton PARSTAT 2273). Galvanostatic charge/discharge measurements (current density: 100 mA/g) were conducted with a charge−discharge tester (Arbin BT2000). The electrochemical capacitances were obtained both from charge−discharge curves (for cycling profile) and CV curves (for capacitance-scanning rate profile), and the details are presented in the Supporting Information.

Acknowledgment. We appreciate the support from National Natural Science Foundation of China (No. 50842060 and 50972101), NSF of Tianjin, China (No. 07JCYBJC15200), Foundation of State Key Laboratory of Coal Conversion (Grant No. 08-913), and Program of Introducing Talents of Discipline to Universities (No. B06006), China.

Supporting Information Available: A digital photograph and configuration of a test cell for electrochemical measurements and cycling performance of low-temperature exfoliated graphenes with organic system. This material is available free of charge *via* the Internet at http://pubs.acs.org.

REFERENCES AND NOTES

1. Geim, A. K.; Novoselov, K. S. The Rise of Graphene. *Nat. Mater.* **2007**, *6*, 183–191.
2. Yan, Q.; Huang, B.; Yu, J.; Zheng, F.; Zang, J.; Wu, J.; Gu, B. L.; Liu, F.; Duan, W. Intrinsic Current−Voltage Characteristics of Graphene Nanoribbon Transistors and Effect of Edge Doping. *Nano Lett.* **2007**, *7*, 1469–1473.
3. Blake, P.; Brimicombe, P. D.; Nair, R. R.; Booth, T. J.; Jiang, D.; Schedin, F.; Ponomarenko, L. A.; Morzov, S. V.; Gleeson, H. F.; Hill, E. W.; *et al*. Graphene-Based Liquid Crystal Device. *Nano Lett.* **2008**, *8*, 1704–1708.
4. Wang, X.; Zhi, L.; Mullen, K. Transparent, Conductive Graphene Electrodes for Dye-Sensitized Solar Cells. *Nano Lett.* **2008**, *8*, 323–327.
5. Stankovich, S.; Dikin, D. A.; Dommett, G. H. B.; Kohlhaas, K. A.; Zimney, E. J.; Stach, E. A.; Piner, R. D.; Nguyen, S. T.; Ruoff, R. S. Graphene-Based Composite Materials. *Nature* **2006**, *420*, 282–286.

6. Novoselov, K. S.; Jiang, D.; Schedin, F.; Booth, T. J.; Khotkevich, V. V.; Morozov, S. V.; Geim, A. K. Two-Dimensional Atomic Crystals. *Proc. Natl. Acad. Sci. U.S.A.* **2005**, *102*, 10451–10453.
7. Zhou, S. Y.; Gweon, G. H.; Fedorov, A. V.; First, P. N.; Deheer, W. A.; Lee, D. H.; Guinea, F.; Neto, A. H. C.; Lanzara, A. Substrate-Induced Bandgap Opening in Epitaxial Graphene. *Nat. Mater.* **2007**, *6*, 770–775.
8. Pan, Y.; Zhang, P H.; Shi, D.; Sun, J.; Du, S.; Liu, F.; Gao, H. Highly Ordered, Millimeter-Scale, Continuous, Single-Crystalline Graphene Monolayer Formed on Ru (0001). *Adv. Mater.* **2009**, *21*, 2777–2780.
9. Reina, A.; Jia, X. T.; Ho, J.; Nezich, D.; Son, H. B.; Bulovic, V.; Dresselhaus, M. S.; Kong, J. Large Area, Few-Layer Graphene Films on Arbitrary Substrates by Chemical Vapor Deposition. *Nano Lett.* **2009**, *9*, 30–35.
10. Stankovich, S.; Dikin, D. A.; Piner, R. D.; Kohlhaas, K. A.; Kleinhammes, A.; Jia, Y.; Wu, Y.; Nguyen, S. T.; Ruoff, R. S. Synthesis of Graphene-Based Nanosheets *via* Chemical Reduction of Exfoliated Graphite Oxide. *Carbon* **2007**, *45*, 1558–1565.
11. Sidorov, A. N.; Yazdanpanah, M. M.; Jalilian, R.; Ouseph, P. J.; Cohn, R. W.; Sumanasekera, G. U. Electrostatic Deposition of Graphene. *Nanotechnology* **2007**, *18*, 135301.
12. Banerjee, A.; Grebel, H. Depositing Graphene Films on Solid and Perforated Substrates. *Nanotechnology* **2008**, *19*, 365303.
13. Dato, A.; Radmilovic, V.; Lee, Z.; Phillips, J.; Frenklach, M. Substrate-Free Gas-Phase Synthesis of Graphene Sheets. *Nano Lett.* **2008**, *8*, 2012–2016.
14. Jiao, L. Y.; Zhang, L.; Wang, X. R.; Diankov, G.; Dai, H. J. Narrow Graphene Nanoribbons from Carbon Nanotubes. *Nature* **2009**, *458*, 877–880.
15. Dikin, D. A.; Stankovich, S.; Zimney, E. J.; Piner, R. D.; Dommett, G. H. B.; Evmenenko, G.; Nguyen, S. T.; Ruoff, R. S. Preparation and Characterization of Graphene Oxide Paper. *Nature* **2007**, *448*, 457–460.
16. Xu, Y.; Bai, H.; Lu, G.; Li, C.; Shi, G. Q. Flexible Graphene Films *via* the Filtration of Water-Soluble Noncovalent Functionalized Graphene Sheets. *J. Am. Chem. Soc.* **2008**, *130*, 5856–5857.
17. Li, D.; Müller, M. B.; Gilje, S.; Kaner, R. B.; Wallace, G. G. Processable Aqueous Dispersions of Graphene Nanosheets. *Nat. Nanotechnol.* **2008**, *3*, 101–105.
18. Chen, H. Q.; Müller, M. B.; Gilmore, K. J.; Wallace, G. G.; Li, D. Mechanically Strong, Electrically Conductive, and Biocompatible Graphene Paper. *Adv. Mater.* **2008**, *20*, 3557–3561.
19. Kim, K. S.; Zhao, Y.; Jang, H. S.; Lee, Y.; Kim, J. M.; Kim, K. S.; Ahn, J. H.; Kim, P.; Choi, J. Y.; Hong, B. H. Large-Scale Pattern Growth of Graphene Films for Stretchable Transparent Electrodes. *Nature* **2009**, *457*, 706–710.
20. Chen, C. M.; Yang, Q. H.; Yang, Y. G.; Lv, W.; Wen, Y. F.; Hou, P. X.; Wang, M. Z.; Chen, H. M. Self-Assembled Free-Standing Graphite Oxide Membrane. *Adv. Mater.* **2009**, *21*, 3007–3010.
21. McAllister, M. J.; Li, J. L.; Adamson, D. H.; Schniepp, H. C.; Abdala, A. A.; Liu, J.; Herrera-Alonso, M.; Milius, D. L.; Car, R.; Prud'homme, R. K.; Aksay, I. A. Single Sheet Functionalized Graphene by Oxidation and Thermal Expansion of Graphite. *Chem. Mater.* **2007**, *19*, 4396–4404.
22. Schniepp, H. C.; Li, J. L.; McAllister, M. J.; Sai, H.; Herrera-Alonso, M.; Adamson, D. H.; Prud'homme, R. K.; Car, R.; Saville, D. A.; Aksay, I. A. Functionalized Single Graphene Sheets Derived from Splitting Graphite Oxide. *J. Phys. Chem. B* **2006**, *110*, 8535–8539.
23. Wu, Z. S.; Ren, W. C.; Gao, L. B.; Liu, B. L.; Jiang, C. B.; Cheng, H. M. Synthesis of High-Quality Graphene with a Predetermined Number of Layers. *Carbon* **2009**, *47*, 493–499.
24. Boehm, H. P.; Clauss, A.; Fischer, G. O.; Hofmann, U. Z. Adsorption Behaviors of Extremely Thin Carbon Foils. *Anorg. Allg. Chem.* **1962**, *316*, 119–127.
25. Boehm, H. P.; Scholtz, W. Z. Deflagration Point of Graphite Oxide. *Anorg. Alleg. Chem.* **1965**, *335*, 74–79.
26. Chung, D. D. L. Exfoliation of Graphite. *J. Mater. Sci.* **1987**, *22*, 4190–4198.
27. Chung, G. C.; Kim, H. J.; Yu, S. I.; Jun, S. H.; Choi, J. W.; Kim, M. H. Origin of Graphite Exfoliation−An Investigation of the Important Role of Solvent Cointercalation. *J. Electrochem. Soc.* **2000**, *147*, 4391–4398.
28. Chung, D. D. L. Intercalate Vaporization during the Exfoliation of Graphite Intercalated with Bromine. *Carbon* **1987**, *25*, 361–365.
29. Viculis, L. M.; Mack, J. J.; Mayer, O. M.; Hahn, H. T.; Kaner, R. B. Intercalation and Exfoliation Routes to Graphite Nanoplatelets. *J. Mater. Chem.* **2005**, *15*, 974–978.
30. Hummers, W. S.; Offeman, R. E. Preparation of Graphite Oxide. *J. Am. Chem. Soc.* **1958**, *80*, 1339.
31. Meyer, J. C.; Geim, A. K.; Katsnelson, M. I.; Novoselov, K. S.; Booth, T. J.; Roth, S. The Structure of Suspended Graphene Sheets. *Nature* **2007**, *446*, 60–63.
32. Huang, L. M.; Cui, X. D.; Dukovic, G.; O'Brien, S. P. Self-Organizing High-Density Single-Walled Carbon Nanotube Arrays from Surfactant Suspensions. *Nanotechnology* **2004**, *15*, 1450–1454.
33. Vivekchand, S. R. C.; Rout, C. S.; Subrahmanyam, K. S.; Govindaraj, A.; Rao, C. N. R. Graphene-Based Electrochemical Supercapacitors. *J. Chem. Sci.* **2008**, *120*, 9–13.
34. Stoller, M. D.; Park, S.; Zhu, Y.; An, J.; Ruoff, R. S. Graphene-Based Ultracapacitors. *Nano Lett.* **2008**, *8*, 3498–3502.
35. Darmstadt, H.; Roy, C.; Kaliaguine, S. ESCA Characterization of Commercial Carbon Blacks and of Carbon Blacks from Vacuum Pyrolysis of Used Tires. *Carbon* **1994**, *32*, 1399–1406.
36. Gardner, S. D.; Singamsetty, C. S. K.; Booth, G. L.; He, G. R.; Pittman, C. U., Jr. Surface Characterization of Carbon Fibers Using Angle-Resolved XPS and ISS. *Carbon* **1995**, *33*, 587–595.